Catalysis and Mass Transport in Spatially Ordered Enzyme Assemblies on Electrodes

Christian Bourdillon,[1b] Christophe Demaille,[1a] Jacques Moiroux,*[,1a] and Jean-Michel Savéant*[,1a]

Contribution from the Laboratoire d'Electrochimie Moléculaire de l'Université Denis Diderot (Paris 7), Unité Associée au CNRS No. 438, 2 place Jussieu, 75251 Paris, Cedex 05, France, and Laboratoire de Technologie Enzymatique, Unité Associée au CNRS No. 1442, Université de Technologie de Compiègne, B.P. 649, 60206 Compiègne, Cedex, France

Received June 19, 1995[⊗]

Abstract: The antigen–antiboby immobilization technique has been extended, with glucose oxidase and glassy carbon electrodes as an illustrating example, so as to obtain up to 10 active successive monolayers. A slight modification of the technique allows the deactivation of any number of enzyme layers adjacent to the electrode and the deposition on top of the inactivated film of any number of active monolayers. Using these structures and varying the rate of the enzymatic reaction makes it possible to observe the interference of mediator mass transport in the control of the current responses together with the enzymatic reaction. The fact that the thickness of the enzyme monolayers derived from these experiments is the same with all of these film structures demonstrates their high degree of spatial order. The value thus found, 470 Å, as well as the value of mediator partition coefficients close to one and of the diffusion coefficients close to their value in solution indicate the low compactness of the enzyme films. The study also provides a starting point for modulating layer by layer the activity of the enzyme film.

Considerable attention is currently devoted to immobilization of enzymes on electrode surfaces in relation with the development of biosensors and biotechnological processes.[2,3] Chemical attachment and entrapment in polymer matrixes have been used in this purpose. A brief review of these studies was given in ref 4. Since then, several extensions have been described.[5–11]

Another approach has been to utilize antigen–antibody interactions. In pioneering studies,[12,13] such an immunological method was employed to deposit enzymes on a surface that was however not used as an electrode. The method described also did not allow an easy estimation of the number of enzyme monolayers deposited and of their activity. More recently an antibody–antigen method for attaching a single enzyme monolayer on an electrode has been described and illustrated by the deposition of a glucose oxidase monolayer on a glassy carbon surface.[4a]

The method was then extended to layer-by-layer construction of a fully active electrode.[14] Up to eight successive monolayers could then be deposited on the electrode. With relatively high concentrations of the mediator (methanol ferrocene, 0.1 mM) and of glucose (0.5 M), the catalytic cyclic voltammetric plateau current was close to proportionality to the number of enzyme

⊗ Abstract published in *Advance ACS Abstracts*, November 1, 1995.

(1) (a) Université Denis Diderot. (b) Université Technologique de Compiègne.

(2) Turner, A. P. F.; Karube, I.; Wilson, G. S. *Biosensors*; Oxford University Press: Oxford, U.K., 1987.

(3) (a) Simon, H.; Bader, J.; Gunther, H.; Neumann, S.; Thanos, J. *Angew. Chem., Int. Ed. Engl.* **1985**, *24*, 539. (b) Laane, C.; Pronk, W.; Franssen, M.; Veeger, C. *Enzyme Microb. Technol.* **1984**, *6*, 165. (c) Bourdillon, C.; Lortie, R.; Laval, J. M. *Biotechnol. Bioeng.* **1988**, *31*, 553.

(4) (a) Bourdillon, C.; Demaille, C.; Guéris, J.; Moiroux, J.; Savéant, J.-M. *J. Am. Chem. Soc.* **1993**, *115*, 12264. (b) Bourdillon, C.; Demaille, C.; Moiroux, J.; Savéant, J.-M. *J. Am. Chem. Soc.* **1994**, *116*, 10328. (c) Bourdillon, C.; Demaille, C.; Moiroux, J.; Savéant, J.-M. *J. Am. Chem. Soc.* **1993**, *115*, 2.

(5) (a) Ohara, T. J.; Vreeke, M. S.; Battaglini, F.; Heller, A. *Electroanalysis* **1993**, *5*, 825. (b) Ye, L.; Hammerle, M.; Olsthorn, A. J. J.; Schuhmann, W.; Ohara, T. J.; Schmidt, H. L.; Duine, J. A.; Heller, A. *Anal. Chem.* **1993**, *65*, 238. (c) Ohara, T. J.; Rajagopalan, R.; Heller, A. *Anal. Chem.* **1993**, *65*, 3512. (d) Aoki, A.; Heller, A. *J. Phys. Chem.* **1993**, *97*, 11014. (e) Katakis, I.; Ye, L.; Heller, A. *J. Am. Chem. Soc.* **1994**, *116*, 3617. (f) Linke, B.; Kerner, W.; Kiwit, M.; Pishko, M.; Heller, A. *Biosens. Bioelectron.* **1994**, *9*, 151.

(6) (a) Bartlett, P. N.; Cooper, J. M. *J. Electroanal. Chem.* **1993**, *362*, 1. (b) Bartlett, P. N.; Pratt, K. F. E. *Biosens. Bioelectron.* **1993**, *8*, 451. (c) Bartlett, P. N.; Caruana, D. J. *Analyst* **1994**, *119*, 175. (e) Bartlett, P. N.; Birkin, P. R. *Anal. Chem.* **1994**, *66*, 1552.

(7) (a) Hendry, S. P.; Cardosi, M. F.; Turner, A. F. P.; Neuse, E. W. *Anal. Chim. Acta* **1993**, *281*, 453. (b) Hale, P.; Lee, H.-S.; Okamoto, Y. *Anal. Lett.* **1993**, *26*, 1. (c) Kaku, T.; Karan, H. I.; Okamoto, Y. *Anal. Chem.* **1994**, *66*, 1231. (d) Geise, R. J.; Rao, S. Y.; Yacynych, A. M. *Anal. Chim. Acta* **1993**, *281*, 467. (e) Battaglini, F.; Calvo, E. J. *J. Chem. Soc., Faraday Trans.* **1994**, *90*, 987.

(8) Wolowacz, S. E.; Yon Hin B. F. Y.; Lowe, C. R. *Anal. Chem.* **1992**, *64*, 1541. (b) Schmidt, H. L.; Gutberlet, F.; Schuhmann, W. *Sens. Actuators, B* **1993**, *13–14*, 366.

(9) (a) Yabuki, S.; Mizutani, F.; Katsura, T. *Sens. Actuators, B* **1993**, *13–14*, 166. (b) Chen, C. J.; Liu, C. C.; Savinell, R. F. *J. Electroanal. Chem.* **1993**, *348*, 317. (c) Harkness, J. K.; Murphy, O. J.; Hitchens, G. D. *J. Electroanal. Chem.* **1993**, *357*, 261.

(10) (a) Yoneyama, H.; Kajiya, Y. *Sens. Actuators, B* **1993**, *13–14*, 65. (b) Kajiya, Y.; Okamoto, T.; Yoneyama, H. *Chem. Lett.* **1993**, 2107.

(11) (a) Willner, I.; Kasher, R.; Zahavy, E.; Lapidot, N. *J. Am. Chem. Soc.* **1992**, *114*, 10963. (b) Katz, E.; Riklin, A.; Willner, I. *J. Electroanal. Chem.* **1993**, *354*, 129. (c) Willner, I.; Riklin, A.; Shoham, B.; Rivenzon, D.; Katz, E. *Adv. Mater.* **1993**, *5*, 912. (d) Willner, I.; Riklin, A. *Anal. Chem.* **1994**, *66*, 1535. (e) Lion-Dagan, M.; Katz, E.; Willner, I. ; Riklin, A. *J. Am. Chem. Soc.* **1994**, *116*, 7913.

(12) (a) Lomen, C. E.; de Alwis, W. U.; Wilson, G. S. *J. Chem. Soc., Faraday Trans. 1* **1986**, *82*, 1265. (b) de Alwis, W. U.; Hill, B. S.; Meiklejohn, B. I.; Wilson, G. S. *Anal. Chem.* **1987**, *59*, 2688.

(13) (a) Another approach was developed for ELISA (enzyme-linked immunosorbent assay) with amperometric detection.[13b,c] Immobilization of the capture antibody onto the carbon electrode surface acting as the immunological solid phase was then followed by sandwich immunological stacking with the analyte (antigen) and an enzyme-labeled antibody. (b) Robinson, G. A.; Cole, V. M.; Rattle, S. J.; Forrest, G. C. *Biosensors* **1986**, *2*, 45. (c) Gyss, C.; Bourdillon, C. *Anal. Chem.* **1987**, *59*, 2350.

(14) (a) The use of avidin–biotin interaction to attach enzymes on surfaces[14b–d,15] offers a strong analogy with the immunological approach. In this connection, the work described in ref 15 bear the strongest similarities with the immunological studies in ref 4. (b) Pentano, P.; Morton, T. H.; Kuhr, W. G. *J. Am. Chem. Soc.* **1991**, *113*, 1832. (c) Pentano, P.; Kuhr, W. G. *Anal. Chem.* **1993**, *65*, 623. (d) Vreeke, M. S.; Rocca, P.; Heller, A. *Anal. Chem.* **1995**, *67*, 303.

(15) (a) Anzai, J.; Hoshi, T.; Osa, T. *Chem. Lett.* **1993**, 1231. (b) Lee, S.; Anzai, J.; Osa, T. *Sens. Actuators, B* **1993**, *12*, 153. (c) Hoshi, T.; Anzai, J.; Osa, T. *Anal. Chem.* **1995**, *67*, 770.

0002-7863/95/1517-11499$09.00/0

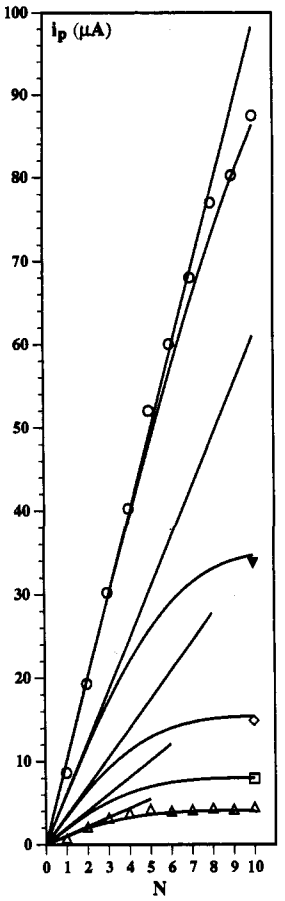

Figure 1. Plateau currents as a function of the number of enzyme monolayers for several concentrations of the ferrocene methanol mediator, C^0 (mM) = 0.2 (○), 0.05 (▼), 0.02 (◇), 0.01 (□), 0.005 (△), in a in pH 8 phosphate buffer (ionic strength = 0.1 M) solution containing 0.5 M glucose. The straight lines are the linear response corresponding to Γ_E^0, $k_3 = 1.2 \times 10^7$ M^{-1} s^{-1}, $k_2 = 700$ s^{-1}, and $k_{red} = 10^4$ M^{-1} s^{-1}. Curved lines show simulation of the interference of mediator mass transport (see text). Scan rate = 0.04 V/s. Temp. = 25 °C.

monolayers, up to eight of them (see Figures 2 and 3 in ref 4b), indicating that each monolayer contains the same amount of active enzyme. The slight downward deviation observed with seven and eight monolayers suggested that mass transport of the mediator through the enzyme film may start to interfere in the overall kinetics governing current response. The deviation was however too small for firm conclusions to be drawn in this respect.

The purpose of the work described below was to investigate in a systematic manner the possible role of mediator mass transport in the control of the current responses. The problem was tackled from different angles. The immunological procedure was extended up to 10 enzyme monolayers so as to enlarge the film thickness, therefore giving more opportunity to mediator mass transport to transpire in the current responses. A much larger range of mediator concentrations was investigated. In the framework of Michaelis–Menten kinetics, a decrease in mediator concentration indeed raises the enzymatic reaction rate relative to the rate of mediator diffusion throughout the film, thus increasing the participation of the latter factor to rate control. Under these conditions, examination of the cyclic voltammetric responses allows a quantitative analysis of the competition between enzymatic reaction and mass transport and therefore an estimation of the thickness of each monolayer. A complementary approach was to modify the procedure for constructing the successive enzyme layers so as to inactivate a prescribed number of them adjacent to the electrode surface and to graft successively one or more active layers. Examining the consistency of the resulting statuses of the competition between enzymatic reaction and mass transport under these conditions and in the case of a film made of active successive layers provides a test of the spatial ordering of the construction.

All the enzyme coatings thus constructed were found to be stable in time with a decrease of enzymatic activity less than 10% over a period of 40 days.

Results and Discussion

The same technique as described in ref 4b was used to deposit successively up to 10 monolayers of glucose oxidase. Plateau-shaped cyclic voltammograms were obtained in the presence of a large glucose concentration (0.5 M) with ferrocene methanol as the mediator that are of the same general type as reported earlier (see Figure 2 in ref 4b).

When the enzymatic reaction is the sole rate-determining step, the plateau current, i_p, is expected to be proportional to the number of monolayers, N, on the electrode. As seen in Figure 1, this situation is met at a relatively high concentration of the mediator ($2\ 10^{-4}$ M). There is a slight downward deviation from proportionality when $N = 9$ and 10, suggesting that the mediator mass transport commences to interfere. Deviation from proportionality is more and more evident and starts earlier and earlier as the concentration of the mediator is decreased (down to 5×10^{-6} M) in accord with a decrease of the rate of the enzymatic reaction relative to the rate of mass transport.

In the absence of mass transport limitations, the plateau current is given by eq 1 in the framework of the following catalytic reaction scheme:

$$P \rightleftarrows Q + e^- \qquad [0]$$

$$FAD + G \underset{k_{-1}}{\overset{k_1}{\rightleftharpoons}} FADG \qquad [I]$$

$$FADG \xrightarrow{k_2} FADH_2 + GL \qquad [II]$$

$$FADH_2 + 2Q \xrightarrow{k_3} FAD + 2P \qquad [III]$$

where P = ferrocene methanol, Q = ferrocenium methanol, G = glucose, GL = gluconolactone, and $FADH_2$ and FAD = reduced and oxidized forms of the flavine adenine dinucleotide enzyme prosthetic group).

$$i_p = \frac{2FSk_3\Gamma_E^0\kappa_Q C^0}{1 + k_3\kappa_Q C^0\left(\frac{1}{k_2} + \frac{1}{k_{red}\kappa_G C_G}\right)}N \qquad (1)$$

where F = faraday, S = electrode surface area, Γ_E^0 surface concentration of enzyme in each monolayer, C^0 = bulk concentration of ferrocene methanol, κ_Q = partition coefficient of ferrocenium methanol from the bathing solution to the enzyme film, N = number of enzyme monolayers, C_G and κ_G = bulk concentration and partition coefficient of glucose, respectively, and k_{red} is defined as

$$k_{red} = \frac{k_1 k_2}{k_{-1} + k_2}$$

Since glucose is present in very large excess, its concentration remains constant an equal to $\kappa_G C_G$ in the film and to C_G in the

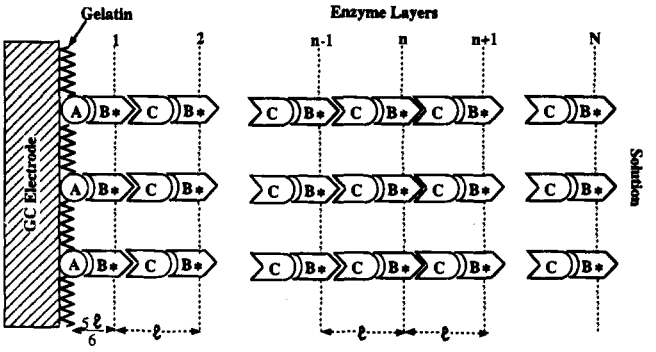

Figure 2. Sketch of the N monolayers of glucose oxidase film on a glassy carbon electrode surface: A, adsorbed mouse IgG (antigen); B, antimouse IgG glucose oxidase conjugate (antibody); C, monoclonal antibody to glucose oxidase produced in mouse. * indicates the approximate location of a glucose oxidase moiety.

solution. The K_M relative to glucose, $K_{M,G} = k_2/k_{red} = 7 \times 10^{-2}$ M, is small. Thus, with such high concentrations of glucose, the enzyme kinetics are practically saturated, i.e., the second term in the denominator parentheses of eq 1 is negligible as compared to the first term. It follows that the value of κ_G does not influence the enzyme kinetics.

In previous studies, the partition coefficient of ferrocenium methanol was tacitly assumed to be unity. The assignment of this value derives from the observation that the values of k_2 and k_{red} found from the "secondary plots" are very close to the solution values.[4a,c] More precisely, the K_M relative to the mediator, $K_{M,Q} = k_2/k_3 = 5.8 \times 10^{-5}$ M, is small. Thus, at high mediator concentrations (0.2−0.4 mM) in the linear region where the current response is controlled by the enzymatic reaction, the value of κ_Q does not influence the enzyme kinetics because the first term in the denominator of eq 1 is negligible as compared to the second term. Upon decreasing the mediator concentration, the downward deviation from proportionality takes place at smaller and smaller values of N. However in the linear section of the i_p−N plot, where the current response is still solely controlled by the enzymatic reaction, eq 1 applies. The first term in the denominator of eq 1 is no longer negligible as compared to the second term, and therefore, the value of κ_Q should influence the enzyme kinetics. The comparison of the slopes observed over the whole range of mediator concentrations then shows that $\kappa_Q = 1$.

Investigation of mediator diffusion through the enzyme film (Figure 2) as a possible rate-limiting factor, together with the enzymatic reaction, requires consideration of the ferrocene methanol partition coefficient, κ_P, and of the diffusion coefficients of both forms of the mediator, D_P and D_Q. In solution, the diffusion coefficients of ferrocene methanol and ferrocenium methanol are the same. Their common value is $D = 6.7\ 10^{-6}$ cm^2 s^{-1}.[16a] In the presence of large amounts of glucose the solution becomes more viscous. With 0.5 M glucose, cyclic voltammetry at a bare glassy carbon electrode revealed that $D = 5.5\ 10^{-6}$ cm^2 s^{-1}.

Information on the partition coefficients may be derived from cyclic voltammetry of the enzyme electrode in the absence of glucose. At low scan rate, the oxidation of ferrocene methanol shows a Nernstian reversible behavior and the voltammograms are practically identical at a bare glassy electrode and at the enzyme electrode (Figure 3). In slow scans, the diffusion layers of P and Q largely exceed the film thickness and therefore the

(16) (a) Ohsawa, Y.; Aoyagni, S. *J. Electroanal. Chem.* **1978**, *86*, 289. (b) The distance l between two successive enzyme monolayers is 6 times the radius of a protein of *ca.* 150 000 molecular weight, whereas in between the electrode and the first monolayer, the distance corresponds approximately to five such radii. This is the reason that l was estimated as $L/(11 - 1/6)$.

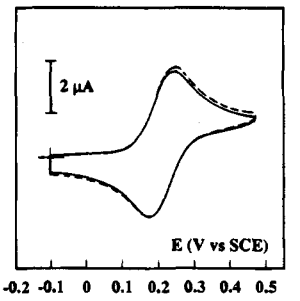

Figure 3. Cyclic voltammetry of ferrocene methanol 0.2 mM in the absence of glucose and in pH 8 phosphate buffer (ionic strength = 0.1 M). Scan rate $v = 0.1$ V/s: (- - -) at a bare electrode, (—) at a glucose oxidase electrode coated with 12 monolayers.

current response is insensitive to the diffusion of the two species within the film. The only manifestation of the presence of the film on the electrode thus derives from the partition coefficients in the relation between the bulk and the electrode concentrations, namely the standard potential in the Nernst law, $E^0_{P/Q}$ at a bare electrode becomes $E^0_{P/Q} + (RT/F)\ \ln(\kappa_P/\kappa_Q)$. Since the peak potentials are the same in the presence and absence of the film we can conclude that $\kappa_P \approx \kappa_Q \approx 1$.

Information concerning the diffusion coefficients within the film may be derived from two sources. One is the catalytic response obtained in the presence of glucose with an electrode where the first $N - 1$ monolayers of enzyme have been deactivated while the Nth layer remains active. The other is examination of the cyclic voltammetry of a set of active layers in the absence of glucose upon raising the scan rate. When the diffusion layer then reaches a size comparable to the film thickness, the magnitude of the mediator diffusion coefficients starts to influence the current response.

The enzymes in the first $N - 1$ monolayers can be deactivated with iodoacetate (see the Experimental Section) under monitoring by the cyclic voltammetric response. When complete deactivation is reached, an active Nth layer is grafted on top of the $N - 1$ inactive layers. We observed that this procedure leads to a surface concentration of enzyme in the Nth layer (as monitored by the catalytic response at high mediator concentration using eq 1 with $N = 1$) which is 60−80% of Γ^0_E, the surface concentration of enzyme per active layer. However when a $(N + 1)^{th}$ active layer is deposited, the surface concentration reaches back Γ^0_E. This is also true for all active layers that can be successively deposited. These results indicate that 20−40% of the enzymes are affected by the chemical deactivation in a way that hampers their recognition by the monoclonal antibodies to glucose oxidase which allows the attachment of the Nth layer. This deficit is however canceled when the $(N + 1)^{th}$ layer is grafted, suggesting that each of the two monoclonal antibodies used in the experiments can recognize two different sites of the same glucose oxidase unit. The reproducible Γ^0_E value, obtained for the $(N + 1)^{th}$ and the successive layers thus corresponds to an optimum in the lateral compactness of each monolayer

Figure 4 shows the variation of the catalytic plateau current with the mediator concentration, in the presence of 0.5 M glucose, with an electrode made of 10 inactivated monolayers and of an eleventh active layer. That the apparently linear reciprocal plot does not merely correspond to a primary plot of the type previously obtained with one monolayer adjacent to the electrode surface[4a] can be shown as follows. At the highest mediator concentration, 0.4 mM, the plateau current is governed solely by the enzymatic reaction and thus eq 1 applies. The reciprocal plot of the plateau current vs mediator concen-

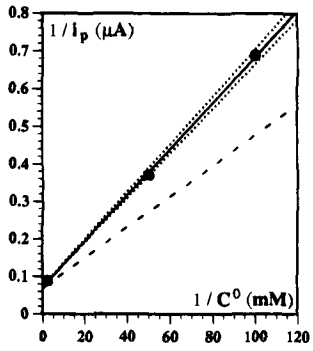

Figure 4. Cyclic voltammetry, in the presence of glucose (0.5 M), of an electrode coated with 10 inactivated enzyme layers ($\Gamma_E^0 = 2.0 \times 10^{-12}$ M/cm^2) and an active eleventh monolayer ($\Gamma_E = 1.5 \times 10^{-12}$ M/cm^2) with ferrocene methanol as mediator in a pH 8 phosphate buffer (ionic strength = 0.1 M). ● shows experimental data. Dashed line shows kinetic control by the enzymatic reaction. Full and dotted lines show simulation of the mixed kinetic control by enzymatic reaction and mediator diffusion (see text).

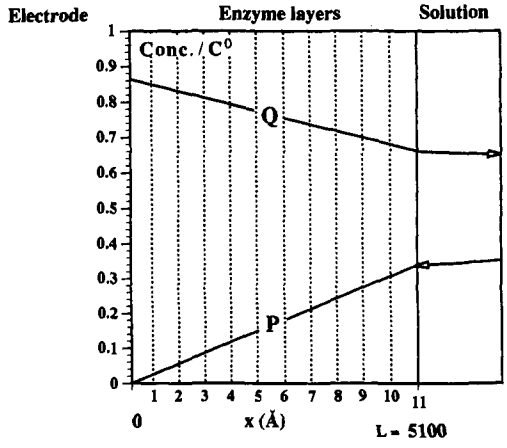

Figure 5. Concentration profiles of the reduced (P) and oxidized forms of the mediator in one of the experiments described in Figure 4 (mediator concentration = 0.01 mM). Vertical dotted lines show inactivated enzyme layers; solid line shows active enzyme layer.

tration that would correspond to the same type of kinetic control, i.e., the primary plot, can be obtained from eq 1 using the same values of the rate constants as before and the value of Γ_E (the actual surface concentration of enzyme, smaller than Γ_E^0) derived from the plateau current at 0.4 mM:

$$\frac{FS}{i_p} = \frac{1}{2\Gamma_E}\left(\frac{1}{k_{red}\kappa_G C_G}\right) + \frac{1}{2k_3\Gamma_E\kappa_Q C^0} \qquad (2)$$

It is represented as a dashed line in Figure 4 (using $k_3 = 1.2 \times 10^7$ M^{-1} s^{-1}, $k_2 = 700$ s^{-1}, and $k_{red} = 10^4$ M^{-1} s^{-1}). It is seen that the experimental points corresponding to lower mediator concentrations stand above the predicted primary plot, indicating the interference of mediator diffusion in the kinetic control of the current response. These results may be analyzed quantitatively as follows. Because the diffusion layer in the solution is much larger than the enzyme film ($\approx 3 \times 10^{-3}$ vs $\approx 5 \times 10^{-5}$ cm as discussed later in more details), the mediator concentration profiles within the film can be considered as linear (Figure 5). Because the enzymatic reaction is fast, resulting in a catalytic plateau current much higher than the one-electron current for the oxidation of the mediator, the flux of Q getting out of the film from the active enzyme layer is negligible in front of the flux entering this layer from the inside of the film. The same is true for the flux of P getting out the active enzyme layer on the film side as compared to the flux entering the active enzyme layer from the solution side.

Thus, inside the film

$$\frac{i_p}{FS} = D_P\frac{(C_P)_{x=L^-} - (C_P)_{x=0}}{L} = D_Q\frac{(C_Q)_{x=0} - (C_Q)_{x=L^-}}{L} = \frac{2k_3\Gamma_E(C_Q)_{x=L^-}}{1 + k_3(C_Q)_{x=L^-}\left(\frac{1}{k_2} + \frac{1}{k_{red}\kappa_G C_G}\right)}$$

with $(C_P)_{x=0} = 0$ (plateau current condition) (the Cs are the concentrations inside the film, $x = L^-$ means that we consider the active enzyme plane on the film side, and $x = L^+$, the active enzyme plane on the solution side). At the film/solution interface

$$(C_P)_{x=L^-} = \kappa_P(C_P)_{x=L^+}, \quad (C_Q)_{x=L^-} = \kappa_Q(C_Q)_{x=L^+}, \text{ and}$$
$$D\left(\frac{\partial C_P}{\partial x}\right)_{x=L^+} = -D\left(\frac{\partial C_Q}{\partial x}\right)_{x=L^+} \approx 0$$

Therefore $(C_P)_{x=L^+} + (C_Q)_{x=L^+} = C^0$ and thus

$$\frac{(C_P)_{x=L^-}}{\kappa_P} + \frac{(C_Q)_{x=L^-}}{\kappa_Q} = C^0$$

Appropriate combination of the above equations then leads to

$$\frac{FS}{i_p} = \frac{1}{2\Gamma_E}\left(\frac{1}{k_2} + \frac{1}{k_{red}\kappa_G C_G}\right) + \frac{1}{2k_3\Gamma_E\kappa_Q C^0\left(1 - \frac{i_p}{FS}\frac{L}{\kappa_P\delta_P DC^0}\right)} \qquad (3)$$

The difference with the primary plot (eq 2) resides in the bracketed term in the denominator of the right-hand member of eq 3. This equation was applied to the data points in the experiment in Figure 4 (using $k_3 = 1.2 \times 10^7$ M^{-1}s^{-1}, $k_2 = 700$ s^{-1}, and $k_{red} = 10^4$ M^{-1} s^{-1}) leading to a best-fit value of $L/\kappa_P\delta_P = 8500$ Å ($\delta_P = D_P/D$ is the ratio of the diffusion coefficients of P inside and outside the film). The thickness of each monolayer, l, is related to the total film thickness, L, by $l = L/(11 - 1/6)$. Therefore, $l/\kappa_P\delta_P = 785$ Å.[16b] The two dotted lines below and above the best-fit line in Figure 4 correspond to $L/\kappa_P\delta_P = 9210$ and 7730 Å, respectively.

As seen before, $\kappa_P \approx 1$. We will see later on, based on further independent experiments, that $\delta_P \approx 0.6 \pm 0.1$. Thus $L = 5100 \pm 1300$ Å and $l = 470 \pm 120$ Å.

It may be noticed that the current response, as expressed by eq 3, involves a parameter, $\kappa_P\delta_P$, characterizing the diffusion of P across the enzyme film and not $\kappa_Q\delta_Q$ characterizing the diffusion of Q. The physical reason behind this mathematical result is that the flux of P at the electrode surface is converted into a diffusion flux of Q that remains constant throughout the film and is eventually used up entirely in the enzymatic reaction at the active enzyme layer located at the film/solution interface.

The mediator concentration profiles can also be derived from the above equations leading to

$$\frac{C_Q}{C^0} = \frac{i_p}{FS\delta_P DC^0}x \quad \text{and}$$
$$\frac{C_Q}{C^0} = \kappa_Q\left[1 - \frac{i_p L}{FSDC^0}\left(\frac{1}{\kappa_Q\delta_Q}\right)\right] - \frac{i_p}{FS\delta_Q DC^0}x$$

where i_p is given by eq 3. The concentration profiles for $C^0 =$

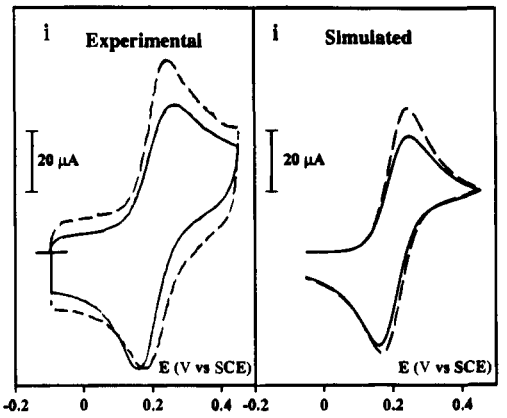

Figure 6. Cyclic voltammetry of ferrocene methanol 0.2 mM in the absence of glucose and in pH 8 phosphate buffer (ionic strength = 0.1 M) at a bare electrode (- - -) and at a glucose oxidase electrode coated with 12 monolayers (—). Experimental and simulated voltammograms at 20 V/s. Parameters for the simulation: $\kappa_P = \kappa_Q = 1$, $\delta_Q = 1$, $\delta_P = 0.6$, $(l/\delta_P)(Fv/RTD)^{1/2} = 8.5 \times 10^{-2}$, $\alpha = 0.5$. $k_S = 0.19$ cm/s for the bare electrode and 0.13 cm/s for the enzyme-coated electrode.

0.01 mM are shown in Figure 5. At the highest mediator concentration, 0.4 mM, where the enzymatic reaction is rate determining, the concentration of P is zero, and the concentration of Q equal to $\kappa_Q C^0$ throughout the film. The comparison we made earlier of the thicknesses of the film and of the diffusion layer in solution ($\approx 5 \times 10^{-5}$ vs $\approx 3 \times 10^{-3}$ cm) was based on the above estimation of L and on an estimate of the diffusion layer as $(\pi DRT/Fv)^{1/2}$. Therefore, at the film solution boundary, the fluxes in solution are *ca.* 50 times smaller than the fluxes on the film side, thus giving support to the neglect of the solution fluxes. The validity of this approximation can be assessed in another manner. Diffusion of P and Q in the solution is described by the following time-dependent equations.

$$(C_P)_{x=L^+} = C^0 - \sqrt{\frac{D}{\pi}} \int_0^t \left(\frac{\partial C_P}{\partial x}\right)_{x=L^+} \frac{d\eta}{\sqrt{t-\eta}}$$

$$(C_Q)_{x=L^+} = -\sqrt{\frac{D}{\pi}} \int_0^t \left(\frac{\partial C_Q}{\partial x}\right)_{x=L^+} \frac{d\eta}{\sqrt{t-\eta}}$$

If diffusion in the solution were to interfere in the current response, this should be time dependent and therefore scan rate dependent. The fact that the voltammograms are plateau-shaped curves not changing with scan rate demonstrates per se the validity of the approximation.

We come now to the determination of the diffusion coefficients of the mediator in the film by means of cyclic voltammetric experiments of electrodes containing layers of active enzyme in the absence of glucose. Upon raising the scan rate, the ratio between the diffusion layer and the film thickness diminishes, entailing the interference of the diffusion across the film in the current response. At the same time, the kinetics of electron transfer at the electrode starts also to influence the cyclic voltammogram as revealed by an increasing gap between the anodic and cathodic peak. A typical example is given in Figure 6 for an electrode coated with 12 monolayers of active enzyme. Starting from the previous observation that $\kappa_P = \kappa_Q = 1$, the current response is a function of the parameters δ_P, δ_Q, and $(l/\delta_P)(Fv/RTD)^{1/2}$ as well as of the kinetics of the electron transfer reaction at the electrode through two parameters, $k_S(RT/FvD)^{1/2}$ (k_S = standard electron transfer rate constant) and α, the transfer coefficient (see the Appendix). The standard electron transfer rate constant at a bare GC electrode was determined from the anodic-to-cathodic peak potential separation[17] (Table 1) and thus found to be $k_S = 0.19$ cm s^{-1}. The deviation from a Nernstian behavior is not sufficient to determine α with much accuracy. In the following discussion α will be taken as equal to 0.5.

Table 1. Determination of the Heterogeneous Charge Transfer Kinetics of the Ferrocene Methanol Mediator Couple[a]

scan rate (V/s)	anodic-to-cathodic peak potential separation (mV)	k_S (cm s^{-1})
2	63	0.23
4	67	0.20
8	72	0.16
20	81	0.165
		av: 0.19 ± 0.05

[a] From the cyclic voltammetry of ferrocene methanol (0.1 mM) in a pH 8 phosphate buffer (ionic strength = 0.1 M) at a bare GC electrode, $\alpha = 0.5$.

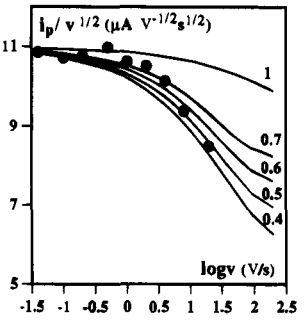

Figure 7. Cyclic voltammetry of ferrocene methanol 0.2 mM in the absence of glucose and in pH 8 phosphate buffer (ionic strength = 0.1 M) at a glucose oxidase electrode coated with 12 monolayers. Experimental (●) and simulated (—) anodic peak current as a function of scan rate. Parameters for the simulation: $\kappa_P = \kappa_Q = 1$, $\delta_Q = 1$, $l/\delta_P = 785$ Å, $k_S = 0.13$ cm/s, $\alpha = 0.5$. The number on each curve is the value of δ_P.

A striking feature of the experimental cyclic voltammogram of the enzyme coated electrode shown in Figure 6 is that the anodic peak current is significantly smaller than the cathodic peak current, the magnitude of the latter being close to the value at the bare electrode. As seen from the simulation in Figure 6, a satisfactory fitting of the experimental curves (taking for l/δ_P the value, 785 Å, derived from the experiment in Figure 4) is obtained for $\delta_Q = 1$ and $\delta_P = 0.6$, with a value of k_S, 0.13 cm s^{-1}, slightly smaller than the value at the bare electrode.[18] Figure 7 describes in more details the variation of the anodic peak current with the scan rate. Simulation then confirms the above assignment of the values of δ_Q and δ_P ($\delta_P = 0.6 \pm 0.1$).

We may now come back to the experiments involving electrodes where the successive enzyme layers are all active such as those summarized in Figure 1 and see if we can simulate the mixed kinetic control by mediator mass transport and enzymatic reaction using the parameters that have just been estimated.

For the same reasons as established before, the concentration profiles of the two forms of the mediator can be regarded as linear in between two successive enzyme layers. Also, the flux of Q getting out of the film from the active enzyme layer can be regarded as negligible in front of the flux entering this layer from the inside of the film, the same being true for the flux of P getting out the active enzyme layer on the film side as compared to the flux entering the active enzyme layer from the

(17) Nicholson, R. S. *Anal. Chem.* **1965**, *37*, 1351.

(18) A reverse situation was observed at pH = 4, where the global charge of the protein system is positive whereas it is negative at pH = 8. The complex interplay of electrostatic interactions and viscosity factors behind these behaviors is not known at present.

solution side. The key equations in the description of the kinetics in the film are those expressing, at each enzyme monolayer, the balance between the diffusion flux entering the layer on one side, the diffusion flux leaving the layer on the other side, and the enzymatic reaction in the enzyme plane. At layer n

$$D_Q\left\{\left(\frac{\partial C_Q}{\partial x}\right)_+ - \left(\frac{\partial C_Q}{\partial x}\right)_-\right\}_n = \frac{2k_3\Gamma_E^0(C_Q)_n}{1 + k_3\left(\frac{1}{k_2} + \frac{1}{k_{red}\kappa_G C_G}\right)(C_Q)_n} = D_P\left\{\left(\frac{\partial C_Q}{\partial x}\right)_- - \left(\frac{\partial C_Q}{\partial x}\right)_+\right\}_n \quad (4)$$

(the subscripts + and − mean right- and left-hand sides, respectively, by reference to the representation given in Figures 5 and 9). Because the concentration profiles are linear in between each enzyme layer, eq 4 translates into

$$D_Q[(C_Q)_{n-1} - 2(C_Q)_n + (C_Q)_{n+1}] = \frac{2k_3\Gamma_E^0(C_Q)_n}{1 + k_3\left(\frac{1}{k_2} + \frac{1}{k_{red}\kappa_G C_G}\right)(C_Q)_n} = D_P[(C_P)_{n+1} - 2(C_P)_n + (C_P)_{n-1}]$$

The concentration profiles and the fluxes at the electrode, given the current, can be easily computed from this series of finite difference equations taking into account the boundary conditions at the electrode:

$$\frac{i_p}{FS} = D_P\frac{(C_P)_1 - (C_P)_0}{(5/6)} = D_Q\frac{(C_Q)_0 - (C_Q)_1}{(5/6)} \quad \text{and}$$

$$(C_P)_0 = 0 \quad \text{(plateau current condition)}$$

and at the film-solution boundary:

$$\frac{(C_P)N}{\kappa_P} + \frac{(C_Q)_N}{\kappa_Q} = C^0$$

where N designates the last layer (see the Appendix for details, introduction of the appropriate dimensionless variables and of the minimal number of parameters that govern the plateau current, and description of the computational procedures).

Besides the mediator concentration, the diffusion coefficient in the solution ($D = 5.5 \times 10^{-6}$ cm^2 s^{-1}), and the characteristic rate constants $k_3 = 1.2 \times 10^7$ M^{-1} s^{-1}, $k_2 = 700$ s^{-1}, and $k_{red} = 10^4$ M^{-1} s^{-1}, the magnitude of the plateau current depends on two dimensionless parameters, $l/\kappa_P\delta_P$ and $\kappa_P\delta_P/\delta_Q$. We thus simulated the plateau currents observed in the experiments summarized in Figure 1 with no adjustable parameters, using for $l/\kappa_P\delta_P$ the value 785 Å derived above from the experiment with 10 inactivated layers and an eleventh active layer (Figure 4). $\kappa_P\delta_P/\delta_Q$ was taken as equal to 0.6, using $\kappa_Q = 1$ from the analysis of the linear sections of the plots in Figure 1, $\kappa_P/\kappa_Q = 1$ from the slow scan experiments in the absence of glucose at a bare and an enzyme-coated electrode (Figure 3), and $\delta_Q \cong 1$ and $\delta_P = 0.6$ from the higher scan rate experiments with the same electrodes (Figures 6 and 7). As seen in Figure 1, there is a good agreement between the experimental and predicted plateau currents. A more detailed picture of the simulation is shown in Figure 8 for the lowest mediator concentration (0.005 M) where the interference of mass transport is maximal. Testing the effect of a variation of $\kappa_P\delta_P/\delta_Q$ confirms that the previous assignement of $\delta_P = 0.6 \pm 0.1$ is correct.

Figure 9 shows the mediator concentration profiles in the enzyme film for a slight ($C^0 = 0.2$ mM) and a strong ($C^0 = 0.005$ mM) participation of mass transport to the kinetics of the current response.

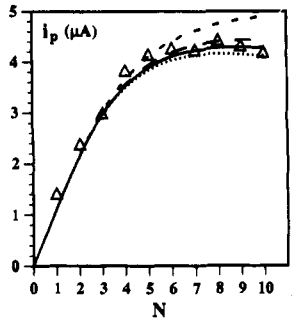

Figure 8. Variation of the plateau current with the number of layers for an electrode coated with active enzyme monolayers with 0.005 mM ferrocene methanol as mediator in a pH 8 phosphate buffer (ionic strength = 0.1 M) in the presence of 0.5 M glucose. $\Gamma^0_{E,n} = 1.6 \times 10^{-12}$ mol/cm^2 Scan rate = 0.04 V/s. Temp = 25 °C. Comparison between experimental data (△) and simulated values for $l/\kappa_P\delta_P = 785$ Å and $\kappa_P\delta_P/\delta_Q = 1$ (- - -), 0.7 (— — —), 0.6 (—) , and 0.5 (•••) (for other parameters, see text).

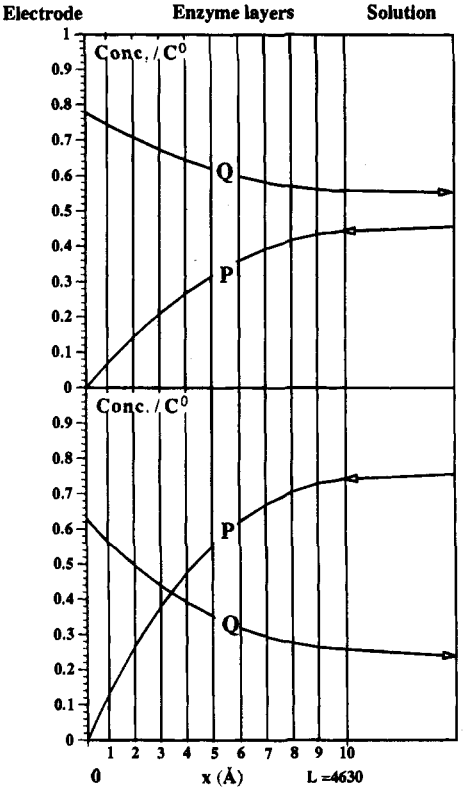

Figure 9. Mediator concentration profiles in the experiments described in Figures 1 and 8 for $C^0 = 0.2$ mM (top) and 0.005 mM (bottom).

The good agreement between the experimental data obtained with a series of active enzyme layers and the simulation based on a layer thickness derived from the experiment with 10 inactivated layer and an eleventh active layer demonstrates that the immunological layer-by-layer construction employed allows a precise spatial ordering of the enzyme film.

This point was confirmed by examining the current responses obtained with an electrode coated with five inactivated monolayers on top of which one to five active monolayers were deposited. As seen in Figure 10, simulation (see the Appendix), again with no adjustable parameters, of the variation of the plateau current with the number of active layers for three different low concentrations of the mediator reproduces satisfactorily the experimental data.

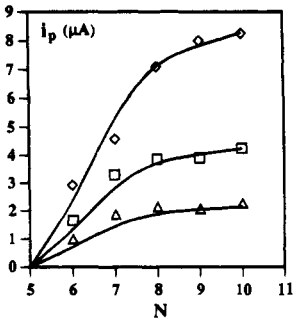

Figure 10. Variation of the plateau current with the number of layers, N, for an electrode coated with five inactivated monolayers ($\Gamma_E = 1.9 \times 10^{-12}$ M/cm^2) and $N - 5$ active layers ($\Gamma_E = 1.15 \times 10^{-12}$ M/cm^2 for the sixth layer and 2.0×10^{-12} M/cm^2 for the seventh, eight, ninth, and tenth layers) with ferrocene methanol as mediator in a pH 8 phosphate buffer (ionic strength = 0.1 M) in the presence of 0.5 M glucose. Scan rate = 0.04 V/s. Temp = 25 °C. $C^0 = 0.02$ (◇), 0.01 (□), and 0.005 (△) mM. Solid line simulation with $l/\kappa_P\delta_P = 785$ Å, $\kappa_P\delta_P/\delta_Q = 0.6$, $k_3 = 1.2 \times 10^7$ M^{-1} s^{-1}, $k_2 = 700$ s^{-1}, $k_{red} = 10^4$ M^{-1} s^{-1}, and $D = 5.5$ 10^{-6} cm^2/s (see text).

Conclusions

The antigen−antibody technique allows the layer-after-layer construction of stable enzyme coatings containing any prescribed number of monolayers. In this manner, up to 10 successive active monolayers have been deposited on the electrode. The technique can also be modified to inactivate a first stack of enzyme layers adjacent to the electrode and then continue to deposit on top of this film one or more active monolayers. These structures give rise, in the presence of glucose and of a mediator, to large catalytic plateau currents in cyclic voltammetry. The systematic analysis of these data as a function of the number of active and inactivated enzyme layers and of the mediator concentration was used to unravel the role of mediator mass transport as a current governing factor together with the kinetics of the enzymatic reaction.

Among the parameters that could be determined from these analyses, the average distance between the enzymatic layers was found to be 475 ± 120 Å. It represents three times the diameter of proteins, including glucose oxidase, of *ca.* 150 000 molecular weight. From ellipsometry and scanning tunneling microscopy data, glucose oxidase appears as an ellipsoid with a 50−80 Å shorter axis and a 140−180 Å longer axis.[19] Assuming that the other proteins present in the construction have comparable dimensions, our estimation of the thickness of one enzyme layer is thus consistent with these data, closer to the highest edge of the range of uncertainty. This observation points to the notion that we are dealing with enzyme films of low compactness thus containing a large proportion of water. It is presumably for the same reason that the partition and diffusion coefficients of the mediator are not very different in the enzyme film and in the bathing solution.

The very fact that the enzyme layer thickness was found to be the same with different film structures containing active and inactivated enzyme layers is a strong indication of the spatial order entailed in its step-by-step construction. A factor which could be vary to a larger extent than done in the present study is the degree of activity of the glucose oxidase conjugate before immobilization. In this manner, the spatial order resulting from the layer-by-layer attachment of the enzyme may be implemented by a modulation of the enzyme activity in each of the monolayers. These possible extension of the technique may prove of interest for future applications to multi-enzymatic systems.

(19) (a) Szucs, A.; Hitchens, G. D.; Bockris, J. O'M. *J. Electrochem. Soc.* **1989**, *136*, 3748. (b) Czajka, R.; Koopal, C. G. J.; Feiters, M. C.; Gerristen, J. W.; Nolte, R. J. M.; Van Kempen, H. *Bioelectrochem. Bioenerg.* **1992**, *29*, 47.

Experimental Section

Chemicals. Chromatography purified rabbit IgG (whole molecule) and mouse IgG (whole molecule) were purchased from Jackson Immuno Research Laboratories. The affinity purified glucose oxidase conjugated antimouse IgG s (whole molecule) was from Organon Teknika Cappel. In the various batches we used, the enzymes had not exactly the same activity leading to somewhat different values of Γ_E^0. The two different kinds of monoclonal antibodies to glucose oxidase, produced in mouse and certified to react with glucose oxidase in solution without altering its enzymatic activity, were from Clonatech and Sigma Immuno Chemicals. All other chemicals were purchased from Aldrich. The stock solutions of glucose were allowed to mutarotate overnight before use. The phosphate buffers for the electrochemical measurements were made of 0.0365 M KH_2PO_4 adjusted to pH 8 with a 1 M NaOH solution leading to an ionic strength of 0.1 M. All solutions were purged from dioxygen before each cyclic voltammetric run.

Successive Immobilization of the Enzyme Monolayers. Solutions of the antigen (0.5 mg/mL), gelatin (0.1 mg/mL), glucose oxidase conjugated antibody (10 μg/mL), and monoclonal antibody to glucose oxidase (40 μg/mL) were all prepared in a buffer composed of 0.01 M KH_2PO_4 and 0.15 M NaCl. The pH was adjusted at 7.4 with a 1 M NaOH solution. In the two latter cases, 0.1 mg/mL of sodium azide was also added to the solution to prevent the formation of bacterial colonies.

The procedure for immobilizing the first monolayer of enzyme was similar to that described in a previous report.[4a] Adsorption of the antigen resulted from a 2 h exposure of the electrode surface to the corresponding solution. The electrode was then thoroughly washed with the buffer and dipped for 10 min in the solution of gelatin. After another thorough washing, the antigen−antibody reaction took place after overnight immersion of the electrode in the solution of glucose oxidase conjugated antibody. This procedure ensures that the first monolayer is saturated with catalytically active glucose oxidase.[4a]

For the immobilization of the next monolayers on top of the first or of any preceding layer we proceeded as follows. The electrode was first immersed in the mouse IgG monoclonal antibody to glucose oxidase solution for 5 h, thus allowing recognition and binding to the glucose oxidase units of the preceding layer. Then, after thorough washing, the electrode thus obtained was left overnight in contact with the glucose oxidase conjugated antimouse IgG. Assays of the total enzymatic activity, as described in the text, showed that no increase of the amount of glucose oxidase thus immobilized resulted from increased immersion times and/or antibody concentrations in each of the two steps of the procedure.

"Thorough washing" consisted in rinsing the electrode with the buffer solution and dipping it in the buffer solution for 30 min.

When not in use, the electrode was stored in the buffer solution containing 0.1 mg/mL NaN_3.

Cyclic Voltammetry Instrumentation. The glassy carbon electrode and the instrument were the same as previously described.[4a,b] The temperature in all experiments was 25 °C.

Appendix

Catalytic Plateau Currents. The following changes in variables and introduction of characteristic parameters, leading to dimensionless formulation of the diffusion/reaction problem, are appropriate for all types of enzyme coated eletrodes that have been considered in this work.

$$q = C_Q/\kappa_Q C^0, \quad p = C_P/\kappa_P C^0$$

$$\lambda = (\kappa_Q l/\kappa_P\delta_P)(k_3\Gamma_E^0/D), \quad \sigma = k_3[(1/k_2) + 1/k_{red}\kappa_G C_G)\kappa_Q C^0$$

$$\varphi = (i/FSDC^0)(l/\kappa_P\delta_P)$$

The most general case corresponds to an electrode coated with N enzyme layers, the first $j-1$ of them are inactive and the following $N-j$ are active as sketched in the scheme below.

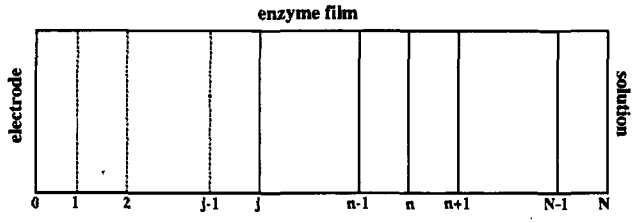

Owing to the linearization of concentration gradients in between two adjacent active or inactive enzyme layers, the following relationships apply as a consequence of the balance of diffusion fluxes and enzymatic reaction:

$$p_0 = 0$$

$$\varphi = \frac{p_1 - p_0}{(5/6)} = -\frac{\kappa_Q\delta_Q}{\kappa_P\delta_P}\frac{q_1 - q_0}{(5/6)}$$

$$(p_2 - p_1) - \frac{p_1 - p_0}{(5/6)} = -\frac{\kappa_Q\delta_Q}{\kappa_P\delta_P}\left[(q_2 - q_1) - \frac{q_1 - q_0}{(5/6)}\right] = 0$$

$$\vdots$$

$$(p_j - p_{j-1}) - (p_{j-1} - p_{j-2}) = -\frac{\kappa_Q\delta_Q}{\kappa_P\delta_P}[(q_j - q_{j-1}) - (q_{j-1} - q_{j-2})] = 0$$

$$(p_{j+1} - p_j) - (p_j - p_{j-1}) = -\frac{\kappa_Q\delta_Q}{\kappa_P\delta_P}[(q_{j+1} - q_j) - (q_j - q_{j-1})] = -\frac{2\lambda q_j}{1 + \sigma q_j}$$

$$\vdots$$

$$(p_{n+1} - p_n) - (p_n - p_{n-1}) = -\frac{\kappa_Q\delta_Q}{\kappa_P\delta_P}[(q_{n+1} - q_n) - (q_n - q_{n-1})] = -\frac{2\lambda q_n}{1 + \sigma q_n}$$

$$\vdots$$

$$-(p_N - P_{N-1}) = \frac{\kappa_Q\delta_Q}{\kappa_P\delta_P}(q_N - q_{N-1}) = -\frac{2\lambda q_N}{1 + \sigma q_N}$$

$$p_N + q_N = 1$$

Combination of the equations belonging to the left-hand column leads to the following relationship between the values of q at the electrode and at the film–solution interface, q_0 and q_N.

$$q_0 = q_N + \frac{\kappa_P\delta_P}{\kappa_Q\delta_Q}(1 - q_N)$$

The set of equations in the right-hand column is then resolved iteratively to obtain the whole set of q values. One may start from a set of q values deriving from the equations in which σ has been taken equal to zero in the denominator of the kinetic terms. This transformation renders each equation linear, and the Gauss elimination method[20] can thus be used to obtain the starting set of q values. These values are then introduce in the denominator of the kinetic term of each equation. The resulting set of linear equations is then resolved by means of the Gauss method leadind to a new set of q values. The procedure is repeated until the relative variation on q_0 is less than 10^{-5}. The plateau current is finally obtained through:

$$\varphi = -\frac{\kappa_Q\delta_Q}{\kappa_P\delta_P}\frac{q_1 - q_0}{(5/6)}$$

Except in the case of one single active monolayer on top of a stack of inactive layers, the calculation of the current depends on the parameters, $\kappa_Q\delta_Q/\kappa_P\delta_P$, $l/\kappa_P\delta_P$, λ, and σ. If Γ_E^0, D, κ_Q, and the rate constants of the enzymatic reaction are known independently, the parameters reduce to $\delta_Q/\kappa_P\delta_P$ and $l/\kappa_P\delta_P$. In the particular case of one single active monolayer on top of a stack of inactive layers, this number of independent parameters is further reduced to one, $l/\kappa_P\delta_P$. In the case of $j-1$ inactive layers and $N-j$ successive active layer, account should be taken of the fact that λ is not the same for the jth layer as for the successive layers since Γ_E is not equal to Γ_E^0.

Cyclic Voltammetry in the Absence of Glucose. In the absence of glucose, the current response results from the diffusion of P and Q in the solution and, when the scan rate is high enough, in the enzyme film with different diffusion coefficient while account should also be taken of the partition coefficients of P and Q. The following changes in variables and introduction of characteristic parameters, leading to a dimensionless formulation of the diffusion, are now appropriate (v = scan rate, t = time, E = electrode potential, $E_{P/Q}^0$ = standard potential of the mediator couple).

$\tau = (Fv/RT)t$ and $\xi = (F/RT)(E - E_{P/Q}^0) = -u + \tau$ with $u = -(F/RT)(E_i - E_{P/Q}^0)$ during the anodic scan starting at E_i, and $\xi = (F/RT)(E - E_{P/Q}^0) = -u' + \tau$ with $u' = -(F/RT)(2E_f - E_i - E_{P/Q}^0)$ during the the reverse cathodic scan starting at E_f, $y = (Fv/RTD)^{1/2}x$, $\epsilon = (N - {}^1/_6)l(Fv/RTD)^{1/2}$, $q = C_Q/C^0$, $p = C_P/C^0$, $\Lambda = k_S(Fv/RTD)^{1/2}$, and $\psi = i/FS(FvD/RT)^{1/2}$. The current can be obtained, through ψ, by numerical resolution of the following set of partial derivative equations and boundary and initial conditions using the Crank–Nicholson finite difference method.

$$\partial p/\partial\tau = \delta_P\partial^2 p/\partial y^2 \qquad \partial q/\partial\tau = \delta_Q\partial^2 q/\partial y^2$$

$$\tau = 0,\ 0 \le y \le \epsilon:\ p = \kappa_P,\ q = 0, \qquad p = 1, q = 0$$

$$y = 0,\ \tau \le 0:\ \psi = \delta_P\partial p/\partial y = -\delta_Q\partial q/\partial y,$$
$$\psi = \Lambda\exp(\alpha\xi)[q - p\exp(-\xi)]$$

$$y = \epsilon,\ \tau \ge 0:\ p_- = \kappa_P p_+,\ q_- = \kappa_Q q_+,$$
$$\delta_P(\partial p/\partial y)_- = (\partial p/\partial y)_+,\ \delta_Q(\partial q/\partial y)_- = (\partial q/\partial y)_+$$

Each dimensionless voltammogram depends separately on the parameters κ_P, κ_Q, δ_P, δ_Q, Λ, and α.

JA9519952

(20) Crank, J. *Mathematics of Diffusion*; Oxford University Press; London, 1964; pp 789–790.